



Effect of Ni on MCM-41 in the Adsorption of Nitrogen and Sulfur Compounds to Obtain Ultra-Low-Sulfur Diesel

Julio César García-Martínez¹ · H. A. González-Uribe¹ · M. M. González-Brambila¹ · N. G. Flores del Río² · A. López-Gaona³ · L. Alvarado-Perea⁴ · J. A. Colín-Luna¹

Published online: 24 July 2018
© Springer Science+Business Media, LLC, part of Springer Nature 2018

Abstract

Adsorption of heterocyclic sulfur and nitrogen compounds like dibenzothiophene (DBT) and quinoline (Q), respectively, was carried out using mesostructured adsorbent MCM-41 and Ni/MCM-41 in calcined (C) and reduced (R) form. These materials were proved in a batch adsorption system using a model fuel diesel: a mixture of dodecane, DBT and Q with the same concentrations of ppmw of sulfur and nitrogen at 313 K and atmospheric pressure. When MCM-41 was impregnated with Ni, an important modification of the adsorption properties was observed, for example, the uptake of DBT was increased and this adsorption was twice in Ni/MCM-41 in reduce form than in the calcined form. On the other hand, for the nitrogen adsorption of Q diminished by 62 and 58%, considering Ni/MCM-41 in reduce form and in calcined form as adsorbent, respectively. This is a significant achievement regarding the desulfurization and denitrogenation, especially for commercial diesel without pretreatment. Moreover, the kinetic results were adjusted with second order considering Q as nitrogen and DBT as sulfur molecule. Data fitting for Q was achieved better by the Langmuir model for all materials than the Freundlich model, meanwhile the experimental adsorption data of DBT was fitted to the Freundlich model for Ni/MCM-41 calcinated and reduced form.

Keywords Dibenzothiophene · Quinoline · Adsorption · Langmuir · Freundlich · Hydrodesulfurization

1 Introduction

Recently worldwide legislation and requirement of ultra-clean transportation fuels e.g. gasoline and diesel have resulted in paying more attention to environmental legislation on the sulfur content in diesel fuel, moreover, has become more stringent because of air pollution by exhaust gas from a diesel engine [1]. The production of ultra-low sulfur diesel (ULSD) is motivated by the need for using new emission-control technologies that are sensitive to sulfur (EURO VI norm). In general, novel catalyst and process have been regarded as the solution for cheaper and cleaner fuel and new technologies like adsorption before the reactor to hydrotreatment (HDT). An alternative to hydrodesulfurization (HDS) is the adsorptive removal of refractory sulfur compounds from fuels like 4,6-dimethyldibenzothiophene, 4-methyldibenzothiophene and dibenzothiophene (DBT) this process shows the advantage of being carried out at moderate conditions. The adsorption process presents the advantage that can be performed at lower conditions of temperature and pressure, and the content of sulfur in fuels can

✉ Julio César García-Martínez
jgarciam@correo.azc.uam.mx

¹ Departamento de Energía, Universidad Autónoma Metropolitana Azcapotzalco, Área de Análisis de Procesos, Av. San Pablo 180, Col. Reynosa, CP. 02200 Mexico City, Mexico

² Maestría en Ciencias de la Ingeniería, Universidad Autónoma de Zacatecas, Campus UAZ Siglo XXI, Carretera Zacatecas-Guadalajara km 6, Ejido La Escondida, CP. 98160 Zacatecas, Mexico

³ Departamento de Química, Universidad Autónoma Metropolitana Iztapalapa, Av. San Rafael Atlixco 186, Col. Vicentina, CP. 09340 Mexico City, Mexico

⁴ Unidad Académica de Ciencias Químicas y Maestría en Ciencias de la Ingeniería, Universidad Autónoma de Zacatecas, Campus UAZ Siglo XXI, Carretera Zacatecas-Guadalajara km 6, Ejido La Escondida, CP. 98160 Zacatecas, Mexico

be reduced to a very low level; moreover, would be integrated into a unitary operation using selective adsorbent materials in adsorption columns before HDT [2, 3]. This approach has the advantage of removing, at the same time, nitrogen basic compounds which are strongly adsorbed on the acidic sites of various catalysts used in petroleum refining processes, resulting in the poisoning of the active sites for the HDS reaction [4, 5]. Moreover, coal-derived liquid fuels contain very high quantities of basic nitrogen containing compounds, including aniline, pyridine, quinoline (Q) and their derivatives [6]. Recently, some studies [7] developed investigations regarding the elimination of DBT and Q with different mesoporous materials like a SBA-15, SBA-16 and MCM-41, showing that the last material presented an advantage over the other two adsorbents.

Since adsorption is based on the concentration of the molecules of a solute (substance to be removed) on the surface of a solid (adsorbent) by the action among its intermolecular forces, so it is easily reversible, representing an advantage for a subsequent desorption [8]. Among various alternatives to achieve the “no sulfur” specification for transportation fuels, adsorptive desulfurization (ADS) is the most promising ultra-deep desulfurization method, because it can be performed at near ambient conditions in absence of hydrogen [9, 10]. The behavior of adsorption and its efficiency of the solid depends on the adsorbent used. To this end, in addition to making a selection based on the structural characteristics of the material, the experimentation is fundamental in order to recognize which material is more convenient for the sulfur-to-nitrogen (S/N) removal considering the adsorbent selective, so it could remove, as well, nitrogen molecules that produces inhibition in HDS reactions [11]. Up to now, some materials have been used for adsorptive desulfurization and denitrogenation, they include activated carbons [8, 11, 12], mesoporous silica, alumina and related materials [13, 14], SBA-15 supported nickel(II) [15] and recently our group proved mesoporous materials like; SBA-15, SBA-16 and MCM-41 [7]. Additionally, to overcome the limitations imposed by micropores with zeolites as adsorbents [16], since large molecules could not interact with the active sites, mesoporous molecular sieves such as MCM-41 and SBA-15 have been studied to adsorb sulfur compounds [7, 17, 18]. Adsorptive desulfurization on the nickel-based sorbents is promising among all new approaches for ultra-deep desulfurization due to high sulfur-adsorption capacity and selectivity [1, 15, 19].

This work is focused on studying new adsorbents to remove nitrogen and sulfur containing-compounds in crude oil hydrocarbons, although we are also proving adsorbents that adsorb DBT compounds from feedstock before HDS unit and try to explain this behavior according to their physicochemical and kinetics properties [7, 20]. In the present research, the adsorption of nitrogen and sulfur

(Q and DBT, respectively) compounds at the same concentration (50, 100, 150, 200 and 250 ppmw) using MCM-41 and Ni/MCM-41 as adsorbents in calcined (C) and reduce (R) form, was carried out in batch mode, considering the nitrogen and sulfur content (190 and 240 ppmw, respectively) agrees well with that found by Silva et al. [21]. In these experiments, kinetic parameters were obtained in presence of both compounds (Q and DBT). Moreover, the equilibrium results were fitted to the corresponding isotherm, Langmuir or Freundlich models.

2 Experimental

2.1 Materials

The MCM-41 material was prepared following the procedure reported by Alvarado Perea et al. [22]. A single procedure was performed as follows: Tetrabutylammonium silicate was prepared with a mixture of 5.4 g of a solution of tetrabutylammonium hydroxide 40 wt% (Sigma-Aldrich) and 0.6 g of silica fumed (Sigma Aldrich). The latter component was mixed with another solution formed by 3.42 g of cetyltrimethylammonium bromide, CTABr (Merck, CTABr $\geq 97\%$) and 23.3 g of deionized water. The resultant mixture was stirred for 15 min; at the end, the mixture had a molar composition of 1 SiO₂:0.35 CTABr:0.31 TBAOH:55 H₂O. That mixture was transferred to a Nalgene bottle and aged for 48 h at 373 K. The resultant solid was recovered by vacuum filtration and washed five times with 250 ml of deionized water each time. The final powder was dried at 353 K for 6 h. At the end, the solid obtained was heated up to 873 K in air at a heating rate of 5 K/min and it was kept at this temperature for 6 h.

Ni/MCM-41 was prepared as follows, using the template ion exchange method reported by Yonemitsu et al. [23]. In a typical experiment 3.0 g of synthesized MCM-41 was mixed with 30 ml of deionized water. To the previous mixture, 30 mL of a solution 0.03 M of Ni²⁺ was added dropwise under vigorous stirring. The Ni precursor was Ni(NO₃)₂·6H₂O $\geq 99.0\%$ from Merck. The resulting mixture was transferred into a Nalgene bottle and treated at 353 K for 20 h without stirring. The solid was recovered by vacuum filtration, washed with deionized water and dried at 353 K for 24 h. The final product was calcinated at 873 K for 6 h in air and the heating rate was 5 K/min, the Ni content is 4.0%, reported by Alvarado Perea et al. [22].

A sample of Ni/MCM-41 was reduced in hydrogen flow of 67 mL/min at 623 K during 1 h. The heating rate was 2 K/min using a fixed bed reactor. After the reduction, the sample was left cool at room temperature using nitrogen.

2.2 Adsorption Experiments

Adsorption experiments were performed in jacketed glass containers at atmospheric pressure and maintaining at 313 K of temperature. All adsorbents were crushed and sifted through 100 mesh sieves. Adsorptive denitrogenation and desulfurization of model nitrogen and sulfur-containing compounds in dodecane were performed using three adsorbents: MCM-41 and Ni/MCM-41 (calcinated (C) and reduced (R) form) in batch mode. The nitrogen and sulfur concentration was fixed between 0 and 250 ppmw (50, 100, 150, 200 and 250) in 40 mL of dodecane, with N/S weight ratio of 1. In each experiment, the mixture was stirred vigorously (400 rpm) until complete homogenization, and at that instant (t_0), a sample was collected in a vial for further analysis in a capillary gas chromatograph (methylphenylsilicone, EC-5 ECONOCAP) with a flame ionization detector (FID) detector. Simultaneously, 0.2 g of adsorbent was added. The samples were collected every 5 min during the first hour and every 15 min for the next two hours; the sample volume was 0.3 mL. The sampling process represents a reduction of the total volume by only around 10%, thus, this volume was considered constant. All samples were filtered to avoid introducing the adsorbent to the gas chromatograph. The adsorption capacities of nitrogen and sulfur compounds were determined using Eq. 1.

$$q_e = \frac{(C_0 - C_e)V}{w} \tag{1}$$

where q_e (mmol/g_{adsorbent}) is the concentration adsorbed of the element (nitrogen or sulfur, considering Q and DBT respectively) at equilibrium per gram of adsorbent, C_0 is the initial concentration of the element (nitrogen or sulfur) in solution (mmol/L), C_e is the equilibrium concentration in solution of nitrogen or sulfur (mmol/L), V is the volume of the solution (L), and w is the weight of the adsorbent (g).

2.3 Adsorption Kinetics

Several models that can adjust the experimental adsorption rate data are found in the literature. Azizian and Fallah [24] have compiled these models. Kinetic models that are commonly used to understand the adsorption process, including a pseudo-first-order model and a pseudo-second-order model, were used to describe the nitrogen adsorption kinetics. The pseudo-second-order model assumes that the rate-limiting step of an adsorption may be chemisorption, which involves valence forces via sharing or electron exchange between the adsorbent and the adsorbate [9, 25]. Pseudo-second-order kinetics can be expressed by the equation below [26].

$$r = \frac{dq}{dt} = k_{ads}(q_e - q)^2 \tag{2}$$

$$\frac{t}{q} = \frac{1}{k_{ads} q_e^2} + \frac{t}{q_e} \tag{3}$$

where q is the amount of nitrogen or sulfur (mmol/g_{adsorbent}) at each time (min), k_{ads} [g/(mmol min)] is the rate constant for pseudo-second-order adsorption, and r is the adsorption rate. q_e has been defined in the previous section. The slopes and intercepts of the linear plots of t/q against t give the values of $1/q_e$ and $1/(k_{ads}q_e^2)$, respectively. Moreover, q_e and k_{ads} can be obtained from the slope and intercept. A correlation factor R^2 close to unity indicates that the process follows the proposed.

2.4 Adsorption Isotherms

The Langmuir isotherm is the most common model used to quantify the amount of adsorbate on the surface of the adsorbent as a function of partial pressure or concentration at a given temperature. It quantitatively describes the formation of a monolayer adsorbate on the outer surface of the adsorbent and no further adsorption can take place, moreover, this isotherm is valid for monolayer adsorption onto a surface containing a finite number of identified sites. The model assumes uniform energies of adsorption on the surface without transmigration of the adsorbate in the plane of the surface. The Langmuir equation governs the adsorption of nitrogen—or sulfur—containing Q or DBT [8], respectively, and its linear form is given as:

$$q_e = \frac{q_m K_L C_e}{1 + K_L C_e} \tag{4}$$

$$\frac{C_e}{q_e} = \frac{1}{q_m K_L} + \frac{C_e}{q_m} \tag{5}$$

where q_m (mmol/g_{adsorbent}) is the Langmuir constant representing the maximum monolayer capacity and K_L is the Langmuir constant equilibrium related to the constant of adsorption and desorption (k_{ads}/k_{des}). C_e and q_e were defined in Sect. 2.2. The slope and intercept of a linear plot of C_e/q_e against C_e yield values of $1/q_m$ and $1/(q_m K_L)$, respectively.

The Freundlich isotherm is an empirical equation employed to describe heterogeneous systems and multilayer adsorption. This isotherm can be expressed by the following equations:

$$q_e = K_F C_e^{1/n} \tag{6}$$

$$\ln q_e = \ln K_F + \frac{1}{n} \ln C_e \tag{7}$$

where K_F and n are Freundlich constants. K_F ($L^{1/n}$ mmol^{(n-1)/n}/g_{adsorbent}) is the adsorption capacity of the sorbent, where n indicates the favorability of the adsorption

process. The magnitude of the exponent $1/n$ gives an indication of the variability of adsorption. Values of $1/n > 1$ represent favorable adsorption conditions and value of $1/n < 1$ implies an unfavorable adsorption chemisorption process [27]. Furthermore, C_e and q_e were defined in Sect. 2.3. To determine the constants K_F and $1/n$, the linear form of the equation may be used to produce a graph of $\ln q_e$ versus $\ln C_e$, where the slope represents $\ln K_F$ and the intercept of the plot represent $1/n$.

3 Results and Discussion

3.1 Adsorption on MCM-41

Figure 1 shows the variation of the nitrogen concentration versus time at different initial concentrations in the batch adsorption of Q at 313 K and atmospheric pressure using MCM-41 as adsorbent. These results reveal fast uptake of adsorbate species at the initial stages of the contact period (< 5 min) and much slower for a longer time. Approximately 90% of the nitrogen was removed in the first 10 min, which means a very high rate of adsorption in a short time, and a steady state was approached. At low concentrations of nitrogen (50 and 100 ppmw N), the steady state was achieved in 20 min.

On the other hand, during the kinetics study, the adsorbate uptake rate was determined with MCM-41. The adsorption kinetics of Q in the presence of DBT in the model diesel fuel is shown in Fig. 2. The results presented a better fit to the second-order kinetic model (Eq. 2) than the first order. For further evaluation, these data were adjusted with the

linearized equation of the model (Eq. 3), in all cases the correlation coefficients (R^2) were near to 1.0 for the pseudo-second-order. According to this Figure, the slope and the intercept at 50 ppmw of N were the highest and decreased when the nitrogen content was increased.

Since the correlation coefficients were closed to the unity, the parameters calculated from kinetic models are summarized in Table 1, indicate that the adsorption behavior of Q can be described appropriately by the pseudo-second-order kinetic in the same way than Shahriar et al. [15]. One may also note that the theoretical adsorption capacity expressed by the kinetic constant of adsorption (k_{ads}) at the initial concentration of 50 ppmw of N presented the value of $3.40 \text{ g}_{adsorbent}/\text{mmol min}$ and decreased when nitrogen content was increased (42% at 100 ppmw) but when increasing the nitrogen content at 150 ppmw increased 24%, presenting the high value at 250 ppmw of N increasing 187% than 50 ppmw N. Moreover, the adsorption rate increased when the nitrogen content increased, showing the maximum value at 250 ppmw of N ($r = 45.05 \text{ mmol/g}_{adsorbent} \text{ min}$), which presented a 98% increase relative to that at 50 ppmw. This may be attributed to the high gradient concentration of nitrogen and content. Finally, the major removal of nitrogen was observed at low concentrations, and the adsorption reduced as the nitrogen content increased.

Thus far, the discussion of the results has been focused on the adsorption of nitrogen because it seems that the mesoporous materials used are capable of adsorbing selectively Q from a mixture of nitrogen and sulfur compounds. Thus, we can conclude that MCM-41 as adsorbent can adsorb Q as nitrogen molecule more than DBT. To support this conclusion, the variation in the sulfur concentration

Fig. 1 Variation of nitrogen concentration at different initial concentrations with a ratio S/N = 1, using MCM-41 as adsorbent: (a) 50 ppmw, (b) 100 ppmw, (c) 150 ppmw, (d) 200 ppmw and (e) 250 ppmw of N. Solid lines correspond to second order model

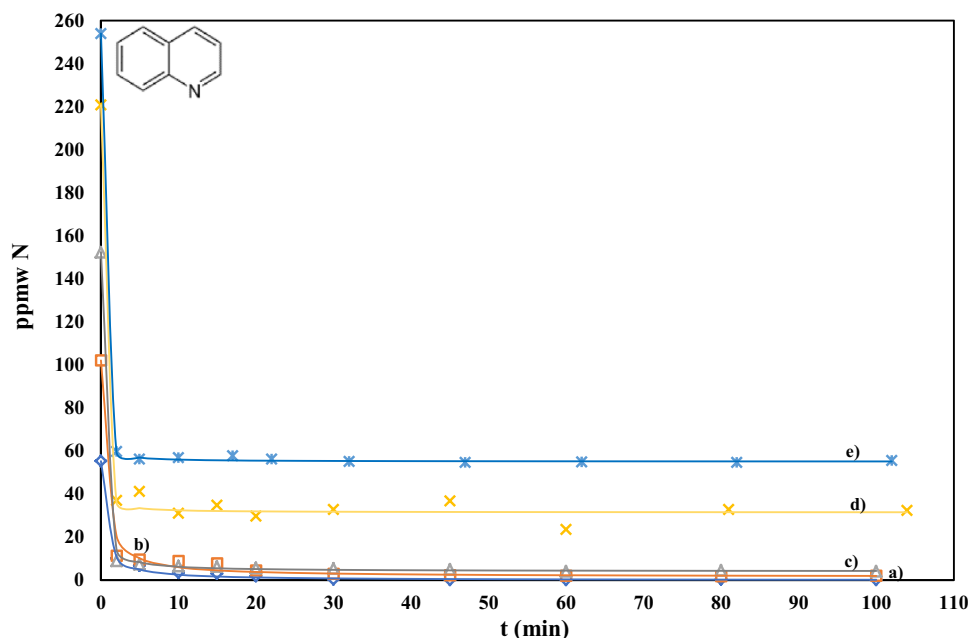


Fig. 2 Kinetic analysis utilizing second order at different initial concentrations with S/N = 1, using MCM-41, (a) 50 ppmw, (b) 100 ppmw, (c) 150 ppmw, (d) 200 ppmw and (e) 250 ppmw of N in presence of DBT. Solid lines are theoretical results with second order analysis

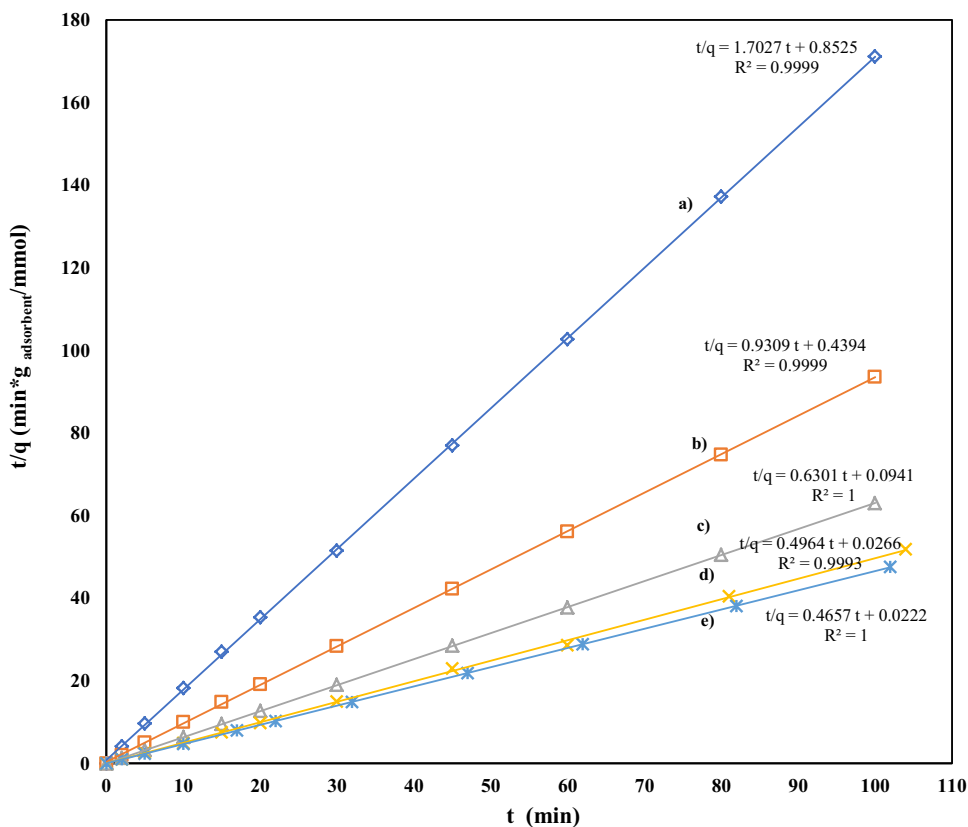


Table 1 Kinetics adsorption results with MCM-41 of Q in presence of DBT in the same amounts

ppmw N	k_{ads} (g _{adsorbent} /mmol min)	r (mmol/g _{adsorbent} min)	% removal
50	3.40	1.17	97.8
100	1.97	2.28	97.1
150	4.22	10.63	97.2
200	9.26	37.59	85.7
250	9.77	45.05	78.3

versus time at different initial concentrations, in the presence of nitrogen, was presented in Fig. 3. Almost no sulfur was adsorbed by MCM-41, and the initial concentration of sulfur did not change during the experiment (100 min) at any initial concentration of sulfur. This result can be relevant because it is known that nitrogen-containing compounds poison the active sites of the catalysts used in the HDS process. Therefore, the selective adsorption of nitrogen molecule in the presence of sulfur compound becomes relevant with this kind of adsorbent. The high surface area and wide pore diameter of MCM-41 is one of the main factors in the adsorption of this basic molecule. The hypothesis that we have is the possibility that the OH

groups available on the surface of the mesoporous material at these temperatures will function as Brønsted acid sites.

3.2 Adsorption on Calcined Ni/MCM-41(C) as Adsorbent

Considering Ni/MCM-41 (C) as adsorbent, in Fig. 4 shows the changes in the nitrogen concentration versus time at different initial concentrations for the batch adsorption of Q at 313 K and atmospheric pressure. The uptake of adsorbate species was a little lower at the initial stages of the contact period than MCM-41 as adsorbent, and thereafter became much slower. Approximately 90% of the nitrogen was removed in the first 5 min, which signifies a very high rate of adsorption. After 10 min, the steady state was reached at all concentrations in the same way that another adsorbent.

The adsorbate uptake rate with Ni/MCM-41 (C) was determined from the adsorption kinetics. The adsorption kinetics parameters of Q in the presence of DBT in model diesel fuel can be estimated from linear form of the second order kinetic given by Eq. (3). The values of slope and intercept are shown in Fig. 5, according with this results slope and intercept were higher than MCM-41 as adsorbent. The correlation coefficients (R^2) were close to the unity for the pseudo-second-order model, in the same way that is observed in Fig. 3 with MCM-41 as adsorbent.

Fig. 3 Variation of the sulfur concentration with time at different initial concentrations, (a) 50 ppmw, (b) 100 ppmw, (c) 150 ppmw, (d) 200 ppmw and (e) 250 ppmw of S, using MCM-41. Solid lines correspond to the second order model

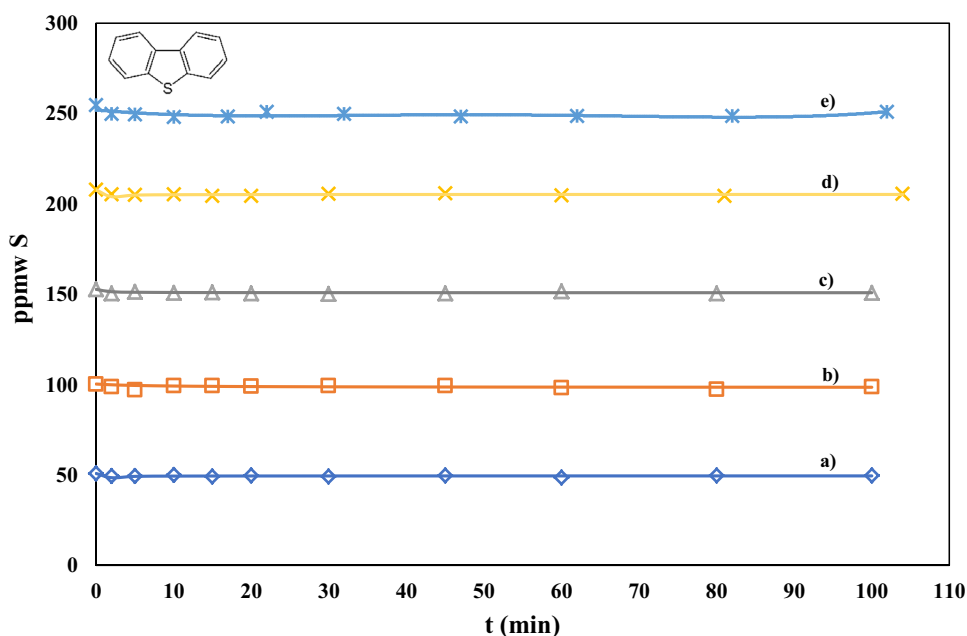
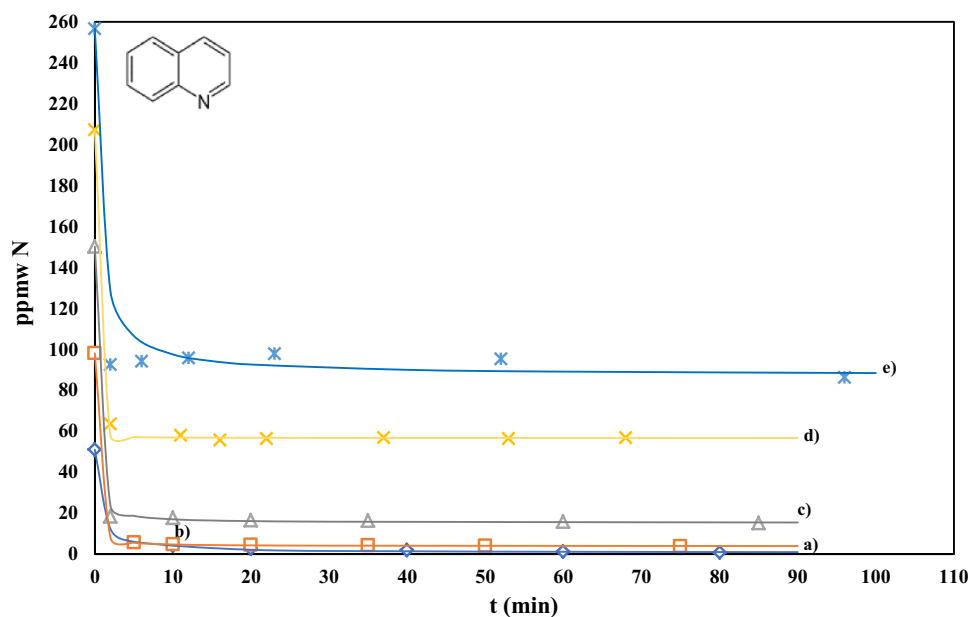


Fig. 4 Variation of nitrogen concentration versus time at different initial concentrations with a ratio $S/N = 1$, using Ni/MCM-41 (C) as adsorbent, (a) 50 ppmw, (b) 100 ppmw, (c) 150 ppmw, (d) 200 ppmw and (e) 250 ppmw of N. Solid lines correspond to second order model



The parameters calculated from the kinetic models (Table 2) indicate that the adsorption behavior of nitrogen can be described by the pseudo-second-order model, considering Ni/MCM-41 (C) as adsorbent. Theoretical adsorption values expressed by the kinetic constant of adsorption at the initial concentration of 50 ppmw of nitrogen presented an increase with 100 ppmw of nitrogen, but when decrease at 150 ppmw of N and then presented an increase, showing the maximum value, lastly with nitrogen concentration of 250 ppmw nitrogen, presented the lowest value, the previous effect may be due to the fact that the presence of Ni has an adsorption and desorption of the Q, due to the fact that this

molecule is being adsorbed. Moreover, the rate of adsorption considering the value of adsorption rate (r), shows the lowest value at 50 ppmw of nitrogen and increasing with nitrogen content, but with 250 ppmw of nitrogen diminished the value, this may be due to the adsorption of DBT on the surface of adsorbent. Finally, the major removal of nitrogen was achieved at low concentration, as can be observed without Ni, i.e. MCM-41 alone as adsorbent (Fig. 1).

The main difference that was found was that when using the adsorbent Ni/MCM-41 (C) with MCM-41, it is that in the first one if the DBT and Q are adsorbed at high concentrations in a mixture, meanwhile at low sulfur contents

Fig. 5 Kinetic analysis utilizing second order at different initial concentrations with S/N= 1, using Ni/MCM-41 (C), (a) 50 ppmw, (b) 100 ppmw, (c) 150 ppmw, (d) 200 ppmw and (e) 250 ppmw of N in presence of DBT. Solid lines are theoretical results with second order analysis

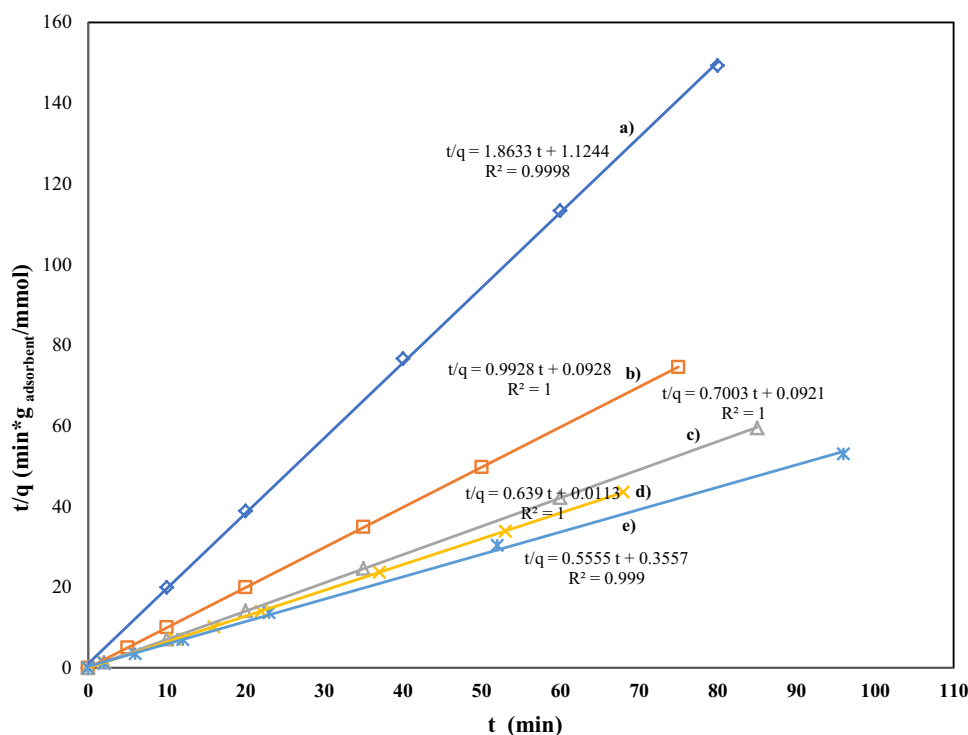


Table 2 Kinetics adsorption results with Ni/MCM-41(C), of DBT in presence of Q

ppmw N	k_{ads} (g _{adsorbent} /mmol min)	r (mmol/g _{adsorbent} min)	% removal
50	3.09	0.89	97.9
100	10.62	10.78	95.8
150	5.32	10.86	89.5
200	36.13	88.50	72.7
250	0.87	2.81	64.9

the DBT is not adsorbed (Fig. 6). Thus, we can conclude that MCM-41 adsorbed selectively nitrogen compound (Q), meanwhile, no sulfur was adsorbed, but when Ni was added at MCM-41 in calcined form (C) as adsorbent, DBT was adsorbed. Therefore, a previously conclusion is that Q is adsorbed preferentially in the support, while DBT gives a possibility that is adsorbed in the metal sites of the Ni at high sulfur content.

3.3 Adsorption on Reduced Ni/MCM-41 (R) as Adsorbent

Figure 7 shows the changes in the nitrogen concentration versus time at different initial concentrations for the batch adsorption of Q in the same conditions that other adsorbents (MCM-41 and Ni/MCM-41(C)), considering Ni-MCM-41 (R). The uptake of adsorbate species was slightly

less pronounced than the other cases. The main difference that should be noted is that after 15 min the steady state was reached at almost all concentrations, unlike with the other two adsorbents. This phenomenon was attributed to the fact that many vacant surface sites are available for adsorption in the initial stage, and hence, the pore arrange of the adsorbent and surface of adsorbent must be considered an important factor.

The adsorption kinetics of Q in the presence of DBT in model diesel fuel utilizing Ni/MCM-41(R) as adsorbent is shown in Fig. 8. The correlation coefficients (R^2) were close to the unity for the pseudo-second-order model in the same way than other experiments with MCM-41 and Ni-MCM-41 (C) and showing the same behavior.

The kinetics parameters with Q in presence of DBT with Ni/MCM-41 (R) are showed in Table 3, according to these results the theoretical adsorption constant at low initial concentration of 50–150 ppmw of nitrogen presented almost the same values, but when increasing the nitrogen content showing the minimum value at 200 ppmw, there is a lower value in the adsorption constant, lastly, at high concentration of 250 ppmw N is more less the same value than Ni/MCM-41(C) this is because the DBT it was adsorbed compared to the MCM-41 as adsorbent. On the other hand, the adsorption rate using Ni/MCM-41 (R) showed orders of magnitude lower with MCM-41 as adsorbent, but with Ni/MCM-41(C) are the same magnitude and the removal was lower than other adsorbents.

Fig. 6 Variation of the sulfur concentration with time at different initial concentrations, (a) 50 ppmw, (b) 100 ppmw, (c) 150 ppmw, (d) 200 ppmw and (e) 250 ppmw of S, using Ni/MCM-41 (C). Solid lines correspond to the second order model

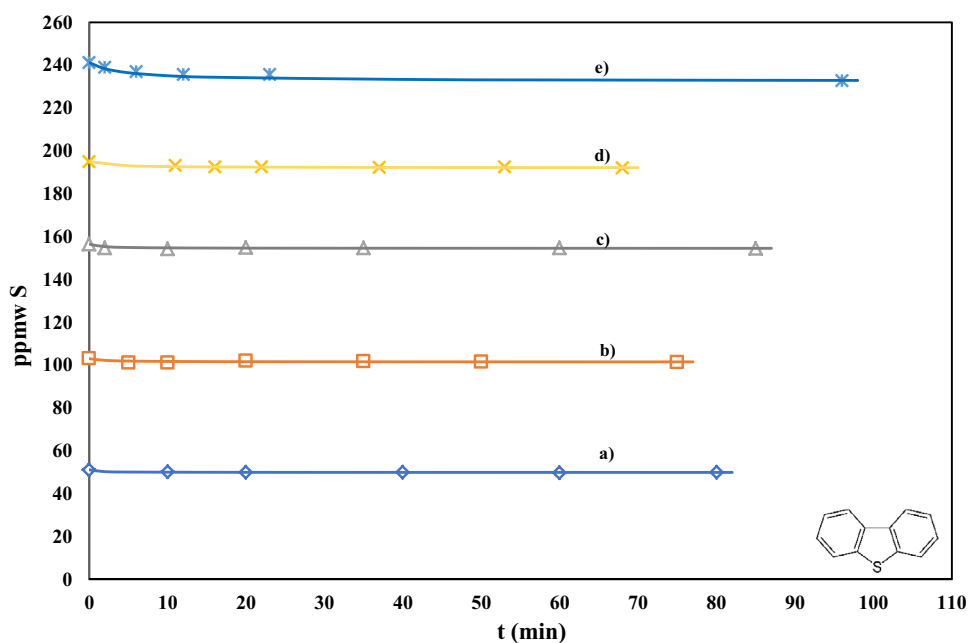
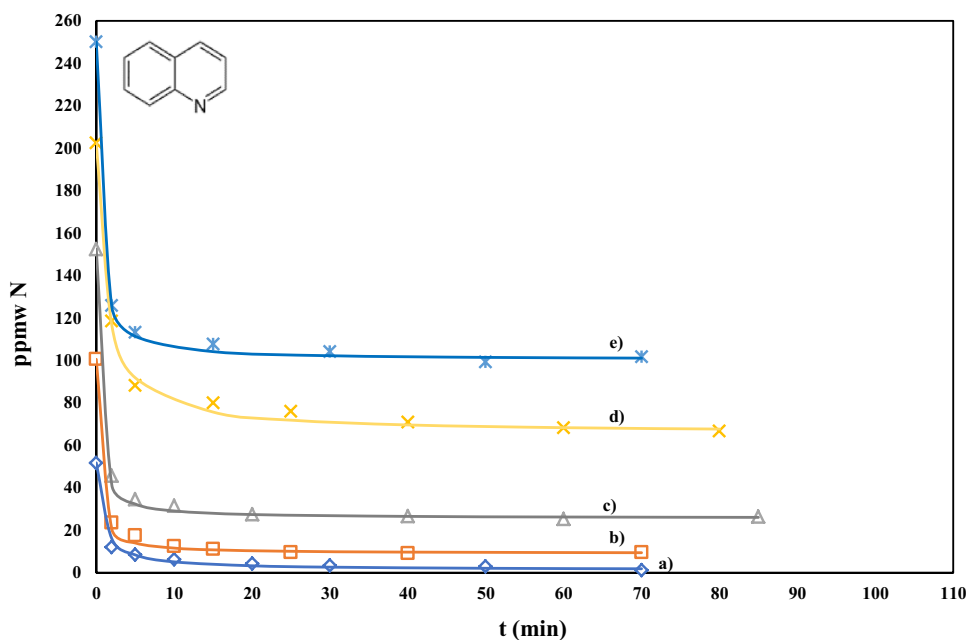


Fig. 7 Variation of nitrogen concentration versus time at different initial concentrations with a ratio S/N = 1, using Ni/MCM-41 (R) reduced as adsorbent, (a) 100 ppmw, (b) 150 ppmw, (c) 200 ppmw and (d) 250 ppmw of N. Solid lines correspond to second order model



So that, the discussion of the results has focused on the adsorption of Q because it seems that the mesoporous materials used are capable of adsorbing only Q from a mixture of Q and DBT with MCM-41. But when adding Ni, the variation in the sulfur amount versus time at different initial concentrations, in the presence of nitrogen using the adsorbent Ni/MCM-41(R), was monitored (Fig. 9) and showing increase of the capacity of adsorption of the DBT at almost concentration of nitrogen was presented than using Ni/MCM-41(C) as adsorbent (Fig. 6). According to the above this would suggest a selective adsorption

between DBT and Q in nickel of sulfur. However, as was shown with MCM-41 (Fig. 1) and Ni/MCM-41 (C) (Fig. 4), the adsorbed amount of Q is practically the same even in presence of DBT. Therefore, the adsorption sites of Q would be on the surface of the MCM-41, whereas those of the DBT would be the metallic sites of the Ni/MCM-41(R), so other effects would cause of the decrease in the capacity of adsorption of Q. This result can be relevant because it is known that nitrogen and sulfur -containing compounds used previous the HDS process with MCM-41 adsorb mainly nitrogen compound like Q [7].

Fig. 8 Kinetic analysis utilizing second order at different initial concentrations with $S/N = 1$, using Ni/MCM-41 (R) reduced, (a) 100 ppmw, (b) 150 ppmw, (c) 200 ppmw and (d) 250 ppmw of N in presence of DBT. Solid lines are theoretical results with second order analysis

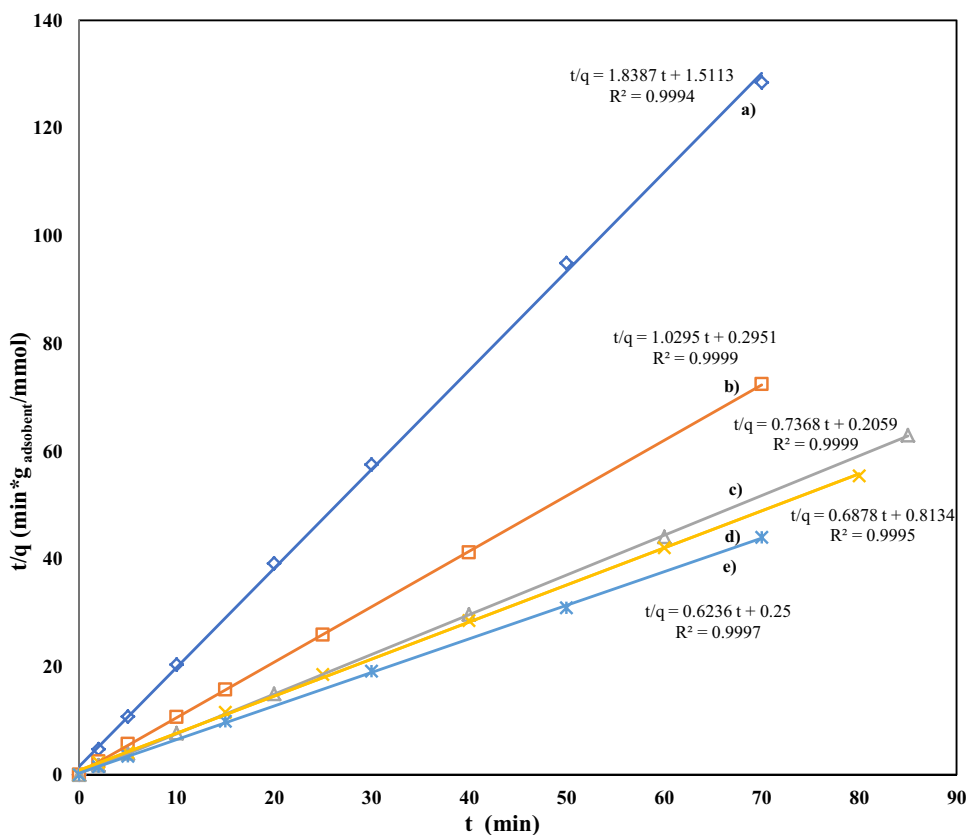


Table 3 Kinetics adsorption results with Ni/MCM-41(R), of Q in presence of DBT

ppmw N	k_{ads} (g _{adsorbent} /mmol min)	r (mmol/g _{adsorbent} min)	% removal
50	2.24	0.66	97.5
100	3.59	3.39	90.6
150	2.64	4.86	82.9
200	0.58	1.23	66.6
250	1.56	4.00	59.0

The adsorbate uptake rate with Ni/MCM-41(R) was determined from the adsorption kinetics, but now the DBT was considered for its analysis. The adsorption kinetics of DBT in the presence of Q in model diesel fuel is shown in Fig. 10. The parameters calculated from kinetic models indicate that the adsorption behavior of DBT in presence of Q can be described appropriately by the pseudo-second-order kinetic model due to correlation coefficients were close to the unity (Fig. 10). In Table 4 shows theoretical adsorption capacity expressed by the kinetic constant of adsorption (k_{ads}), at the initial concentration of 50 ppmw of sulfur presented the highest value and decreased with increasing sulfur content this constant. Moreover, the adsorption rate of sulfur was lower than when Q was used this means that there

is less surface area for the DBT to adsorb in particles of nickel. Lastly, the maximum removal of sulfur was obtained with low value of sulfur content.

3.4 Adsorption Isotherms

3.4.1 Quinoline Adsorption Isotherm

Figure 11 shows the results of equilibrium adsorption against concentration using Q. The dotted lines show the adjustment of the isotherm to the experimental data. This adjustment was using the Langmuir and Freundlich isotherms for the adsorbents used in this research. It can be observed that MCM-41 presented a higher adsorption in comparison to the Ni/MCM-41(C) and Ni/MCM-41(R) as adsorbents. Besides we can observe the best fit was when considering the Langmuir model for all materials, this mean that Q adsorb in a monolayer on the adsorbent.

Besides, Table 5 presents the values obtained from the constants for the isotherm that was adjusted considering the Q adsorption. It is observed that the material MCM-41 presented a bigger value of q_m than the other adsorbents (Ni/MCM-41(C), Ni/MCM-41(R)), the above gives us serves to try to explain that Q is being adsorbed without nickel. Moreover, the Langmuir constant presented the highest value with the MCM-41 material, this helps us

Fig. 9 Variation of the sulfur concentration with time at different initial concentrations in presence of N, (a) 50 ppmw, (b) 100 ppmw, (c) 150 ppmw, (d) 200 ppmw and (e) 250 ppmw of S, using Ni/MCM-41 (R). Solid lines correspond to the second order model

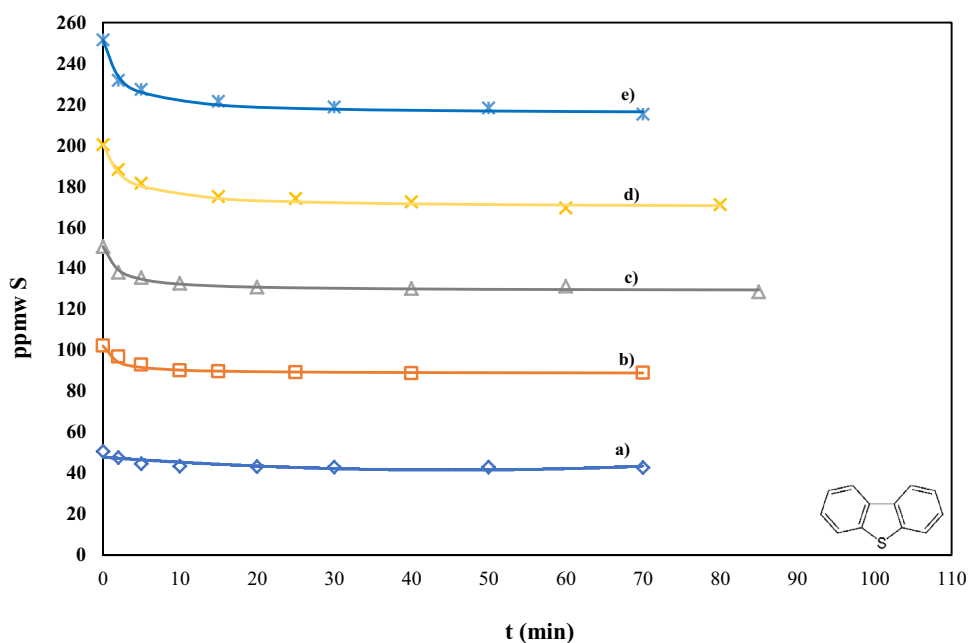
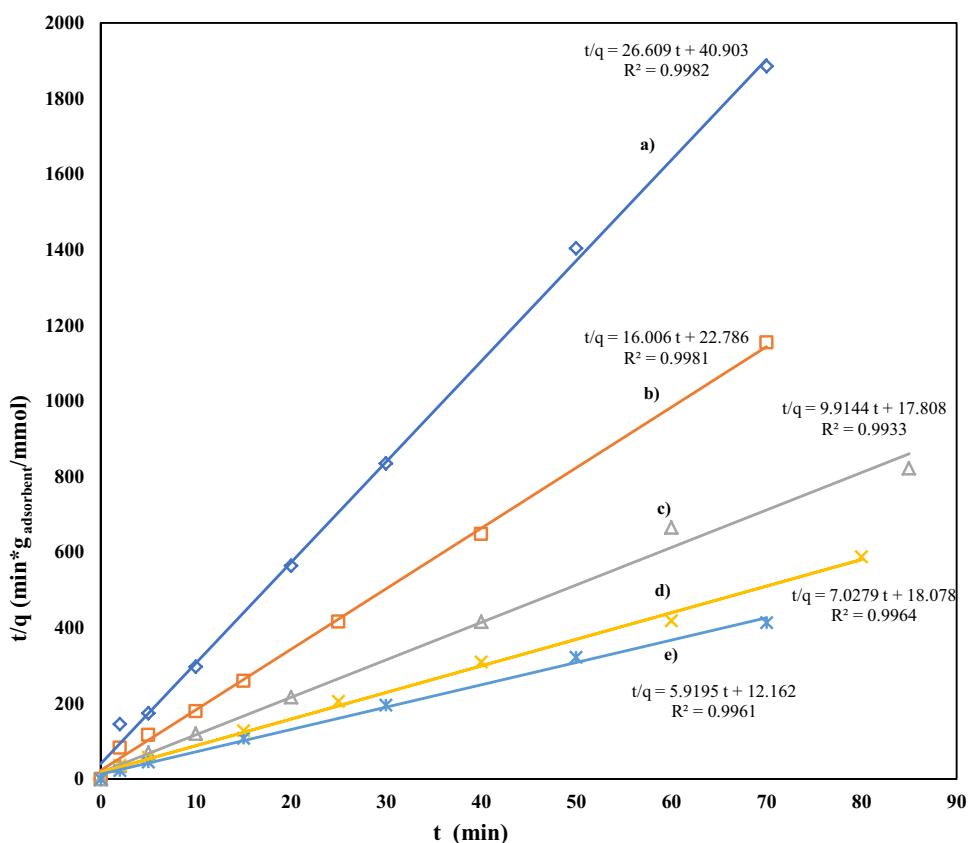


Fig. 10 Kinetic analysis utilizing second order at different initial concentrations with S/N = 1, using Ni/MCM-41 (R), (a) 50 ppmw (b) 100 ppmw, (c) 150 ppmw, (d) 200 ppmw and (e) 250 ppmw of S in presence of N. Solid lines are theoretical results with second order analysis



to think that Q is being adsorbed preferentially and more quickly without Ni, in this table present the equation of Langmuir and correlation factor that was approximated to the unity.

3.4.2 Dibenzothiophene Adsorption Results

Results to describe the adsorption processes of adsorption considering DBT indicate that the Langmuir model did not

Table 4 Kinetics adsorption results with Ni/MCM-41(R) of DBT in presence of Q

ppmw S	k_{ads} ($\text{g}_{\text{adsorbent}}/\text{mmol min}$)	r ($\text{mmol}/\text{g}_{\text{adsorbent}} \text{ min}$)	% removal
50	17.31	0.024	15.8
100	11.24	0.044	12.9
150	5.52	0.056	14.0
200	2.73	0.055	14.8
250	2.88	0.082	13.9

adjust to experimental data, but the Freundlich model is appropriate, which suggests that multilayer adsorption take place for the adsorption of sulfur compound with Ni/MCM-41(C) and Ni/MCM-41 (C) (Fig. 12). Moreover, as can be seen in Table 6 the DBT adsorption process is heterogeneous and infinite surface coverage of the adsorbate occurred without maximum adsorption, which may be considered as multilayer adsorption as follows: if ($1/n = 1$), the adsorption is linear; if ($1/n > 1$), then adsorption is a chemical process and favourable, if ($1/n < 1$), then adsorption is a physical process [27]. The value in Freundlich equation with Ni/MCM-41(C) of $1/n$ was found to be 0.63 indicating the nonlinearity degree of adsorption, but when Ni/MCM-41(R) this value was found to be 1.14, indicating the possible chemical process and favourable adsorption. With these results, we affirm that adsorption of DBT with the adsorbent Ni/MCM-41(R) is higher than with the other two materials.

The observation that reduced Ni/MCM-41(R) exhibits a better sulfur adsorption performance compared to the unreduced material, Ni/MCM-41(C), suggest that

metallic Ni particles dispersed in the structure are more effective than unreduced Ni cation in removing organo-sulfur compound, as it has been mentioned by Velu et al. [28], this behavior could be described according to the proposed diagram shown in Fig. 13. One possible explanation for the above is that the adsorption of DBT to Ni/MCM-41(R) can be explained via sulfur-to metal interaction, π -complexation, and non-specific interactions such as Van der Waals interactions. DBT is a soft base explaining why loading a borderline acid such as nickel to the surface of the Ni/MCM-41(R) could weaken the established acidic sites on the adsorbent's surface, thus, enhancing the adsorption of DBT to a certain extent. Additionally, the two aromatic rings of DBT provide high dispersive interactions between the delocalized π -electrons of DBT and Ni/MCM-41(R). Moreover, the fact that the stability of d^{10} electron configuration in reduced Ni^0 promoted efficiently electron transformation from the d orbital of Ni^0 to the antibonding π^* (antibonding p orbital) of DBT during the formation of $\text{Ni}^0\text{-S}$ or $\text{Ni}^0\text{-}\pi$ bonding in comparison with Q, in the same way that Subhan and Liu [17].

Table 5 Langmuir model parameters for the adsorption isotherms considering Q in presence of DBT with three adsorbents

Adsorbent	q_m (mmol/g)	K_L (L/mmol)	Equation	R^2
MCM-41	2.16	19.09	$q_e = \frac{41.23 C_e}{1+19.09 C_e}$	0.9981
Ni/MCM-41(C)	1.80	5.37	$q_e = \frac{9.66 C_e}{1+5.37 C_e}$	0.9930
Ni/MCM 41(R)	1.65	3.61	$q_e = \frac{5.96 C_e}{1+3.61 C_e}$	0.9970

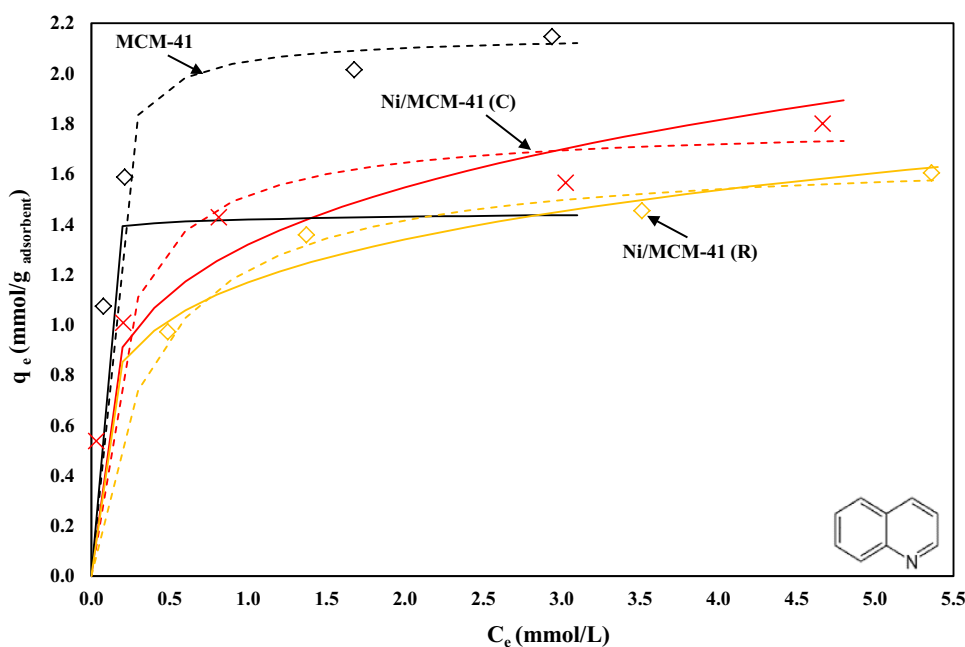
Fig. 11 Adsorption isotherms with MCM-41, Ni/MCM-41 (C) and Ni/MCM-41 (R) with Q in presence of DBT. Dashed lines represent Langmuir model and solid lines Freundlich model


Fig. 12 Adsorption isotherms with Ni-MCM-41 reduced considering S in presence of N. Dashed lines represent Langmuir model and solid lines Freundlich model

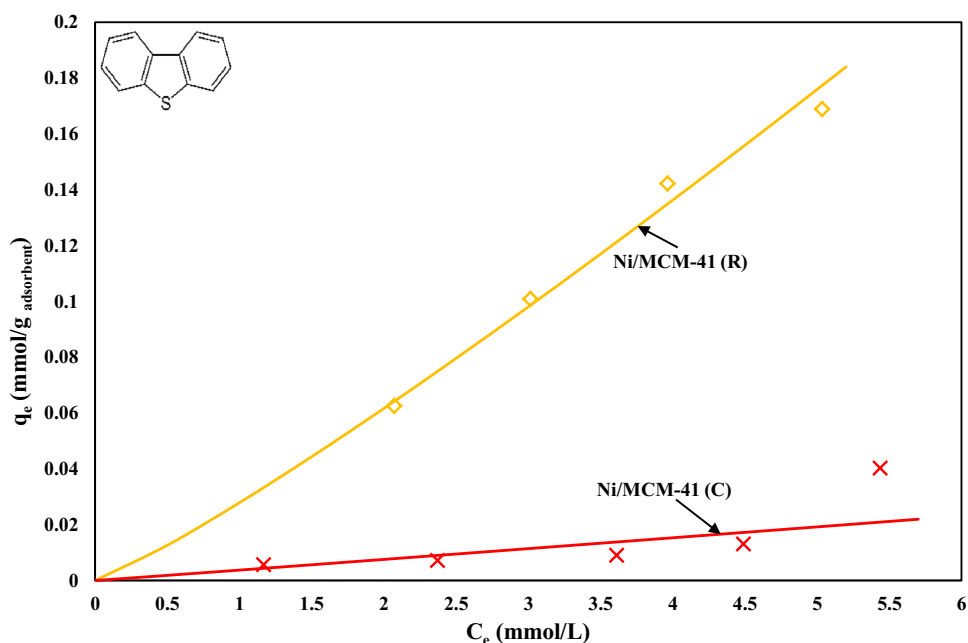


Table 6 Freundlich model parameters for the adsorption of DBT in presence of Q

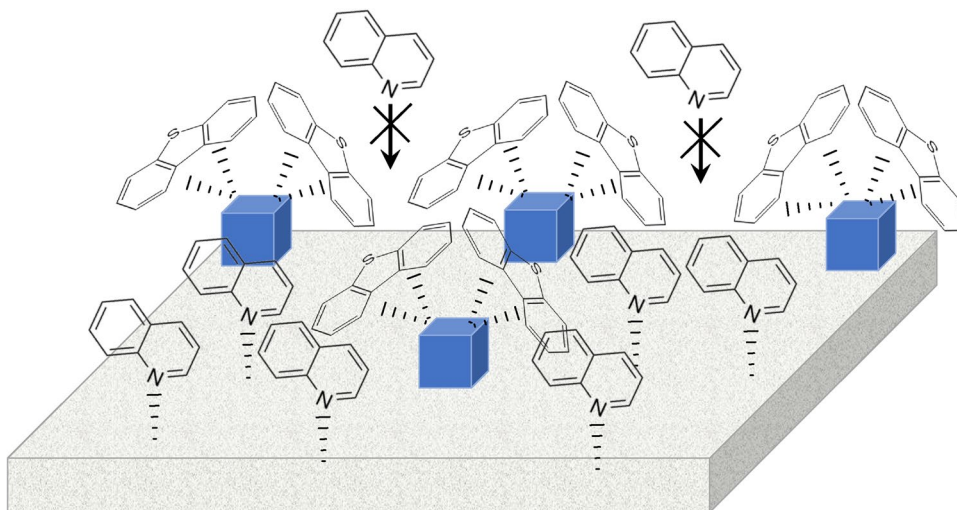
Adsorbent	1/n	K_F (L ^{1/n} mmol ^{(n-1)/n} /g)	Equation	R ²
Ni/MCM-41(C)	0.63	0.0052	$q_e = 0.0052 C_e^{0.63}$	0.9713
Ni/MCM 41(R)	1.14	0.028	$q_e = 0.028 C_e^{1.14}$	0.9889

4 Conclusions

In summary, in this work the adsorption of nitrogen and sulfur compounds using mesoporous Ni based materials

to produce clean fuels was studied, it was found that the adsorption experimental data of Q adjusted to the isotherm of Langmuir with MCM-41 as adsorbent. However, it was determined that MCM-41 adsorbed nitrogen compound, but when adding Ni sulfur compound (DBT) was adsorbed. On the other hand, when using Ni/MCM-41 (R) the capacity of the adsorption process of Q decrease, a possible explanation is that this may be because the Ni sites would block of pore in this material with MCM-41. The most adsorption capacity of Q in MCM-41 it can be explained by the absence of nickel. The sulfur compound (DBT) is expected to be adsorbed by direct sulfur–metal (S–M) interaction over the reduced sample, while their adsorption on the reduced samples may involve π complexation, wherein sulfur adsorption

Fig. 13 Schematic representation of the adsorption sites of Q and DBT on mesoporous material Ni/MCM-41, box blue represents Ni



could be suppressed by the competitive adsorption of nitrogen compounds such as Q present in diesel.

Acknowledgements Julio César García-Martínez would like to thank the Universidad Autónoma Metropolitana Azcapotzalco to the Energy Department and the Programa para el desarrollo profesional Docente (PRODEP) from México.

References

1. Velu S, Ma X, Song CS, Namazian M, Sethuraman S, Venkataraman G (2005) *Energy Fuels* 19:1116–1125
2. Song CS (2003) *Catal Today* 86(1–4):211–263
3. Song CS, Ma XL (2003) *Appl Catal B* 41(1–2):207–238
4. Liu K, Ng FTT (2010) *Catal Today* 149:28–34
5. García-Martínez JC, Castillo-Araiza CO, De los Reyes Heredia JA, Trejo E, Montesinos A (2012) *Chem Eng J* 210:53–62
6. Glauca HCP, Rao Y, Klerk A (2017) *Energy Fuels* 31:14–36
7. García-Martínez JC, González-Urbe HA, González-Brambila MM, Colín-Luna JA, Escobedo-García YE, López-Gaona A, Alvarado-Perea L (2018) *Catal Today* 305:40–48
8. Wen J, Han X, Lin H, Zheng Y, Chu W (2010) *Chem Eng J* 164(1):29–36
9. Jiang J, Ng FTT (2010) *Adsorption* 16:549–558
10. Subhan F, Yang Z, Peng P, Ikram M, Rehman S (2014) *J Hazard Mater* 270:82–91
11. Almarri M, Ma X, Song Ch (2009) *Energy Fuel* 23(8):3940–3947
12. Xiong J, Zhu W, Li H, Yang L, Chao Y, Wu P, Xun S, Jiang W, Zhang M, Li H (2015) *J Mater Chem A* 3:12738–12747
13. Kwon JM, Moon JH, Bae YS, Lee DG, Sohn HC, Lee CH (2008) *ChemSusChem* 1(4):307–309
14. Li Z, Barnes JC, Bosoy A, Stoddart JF, Zink JI (2012) *Chem Soc Rev* 41:2590–2605
15. Shahriar S, Han X, Lin H, Zheng Y (2016) *Int J Chem React Eng* 14(4):823–830
16. Hernández-Maldonado A, Yang R (2003) *Ind Eng Chem Res* 42:123–129
17. Subhan F, Liu BS (2011) *Chem Eng J* 178:69–77
18. Nair S, Tatarchuk B (2010) *Fuel* 89:3218–3225
19. Ma X, Velu S, Kim JH, Song CS (2005) *Appl Catal B* 56:137–147
20. Lee SW, Ryu JW, Min W (2003) *Catal Surv Asia* 7 (4):271–279
21. Silva JMPF, Silveira EB, Costa ALH, Veloso CO, Henriques CA, Zotin FMZ, Paredes MLL, Reis RA, Chiaro SSX (2014) *Ind Eng Chem Res* 53:16000–16014
22. Alvarado-Perea L, Wolff T, Veit P, Hilfert L, Edelmann FT, Hamel C, Seidel-Morgenstern A (2013) *J Catal* 305:154–168
23. Yonemitsu M, Tanaka Y, Iwamoto M (1997) *Chem Mater* 9:2679–2681
24. Azizian S, Fallah RN (2010) *Appl Surf Sci* 256(17):5153–5156
25. Wang L, Wang A (2008) *J Hazard Mater* 160:173–180
26. Ho YS, McKay G (1999) *Process Biochem* 34 (5):451–465
27. Laredo GC, Vega-Merino PM, Montoya-de la Fuente JA, Mora-Vallejo RJ, Meneses-Ruiz E, Castillo JJ, Zapata-Rendon B (2016) *Fuel* 180:284–291
28. Velu S, Song Ch, Engelhard MH, Chin YH (2005) *Ind Eng Chem Res* 44:5740–5749